A R C H I V E S O F M E T A L L U R G Y A N D M A T E R I A L S
Volume 50 2005 Issue 1

K. SZTWIERTNIA* , J. MORGIEL* E. BOUZY**

DEFORMATION ZONES AND THEIR BEHAVIOUR DURING ANNEALING IN 6013 ALUMINIUM ALLOY

STREFY DEFORMACJI I ICH ZACHOWANIE SIĘ W CZASIE WYŻARZANIA W STOPIE ALUMINIUM 6013

The microstructure of cold rolled 6013 aluminum alloy is strongly inhomogeneous; in the laminar matrix are dispersed large (> 1μm) particles of the second phase with zones of localized strain around. The local crystallographic orientation distributions in such regions, determined by measurement of crystallographic orientations in TEM, differ significantly from the global deformation texture. In general, strong dispersed orientations in the zones tends to group in the areas of deformation components after rotation about transverse (TD) or/and normal direction (ND). From the combined calorimetric-microscopic investigations and local orientation measurements (FEGSEM/EBSD) it follows that recrystallization can be considered as a few, partly overlapping processes proceeding in two steps. In the first step, particle stimulated nucleation (PSN) and some enlargement of new grains in the directions of low orientation gradient (mainly in the sheet plane) occur. In consequence the new grains often have a platelike habit with shorter axis parallel to ND. The orientations of the PSN grains are lying among those measured at deformed stage around large particles. In the second step the growth of new grains in the direction of high orientation gradient (here in the ND) is observed; this growth is limited by the distances between large particles along ND.

Mikrostruktura walcowanego na zimno stopu aluminium 6013 jest silnie niejednorodna; w laminarnej matrycy są rozproszone duże (> 1μm) wydzielenia innych faz otoczone strefami zlokalizowanego odkształcenia. Otrzymane w TEM rozkłady lokalnych orientacji krystalograficznych w strefach różnią się istotnie od globalnej tekstury odkształcenia. Silnie rozproszone orientacje mają tendencję do grupowania się w obszarach składowych deformacji po obrocie wokół kierunku poprzecznego (KP) i/lub normalnego (KN). Z badań kalorymetryczno-mikroskopowych oraz pomiarów lokalnych orientacji (FEGSEM/EBSD) wynika, że rekrystalizacja jest superpozycją szeregu lokalnych procesów zachodzących w

* POLISH ACADEMY OF SCIENCES, INSTITUTE OF METALLURGY AND MATERIALS SCIENCE, 25 REYMONTA ST, 30- 059 KRAKOW, POLAND
** UNIVERSITE DE METZ, LABORATOIRE D'ETUDE DES TEXTURES ET APPLICATION AUX MATERIAUX (LETAM), ILE DE SAULCY, 57045 METZ CEDEX 01, FRANCE

dwóch etapach. W etapie pierwszym zachodzi zarodkowanie stymulowane wydzieleniami drugiej fazy, a następnie powiększanie się nowych ziarn w kierunkach niskich gradientów orientacji (głównie w płaszczyźnie blachy). W konsekwencji nowe ziarna mają postać płytek z krótszą osią równoległą do kierunku normalnego. Orientacje nowych ziarn leżą w obszarach orientacji mierzonych w strefach zlokalizowanego odkształcenia wokół wydzieleń. W drugim etapie rekrystalizacji zachodzi wzrost nowych ziarn w kierunkach dużych gradientów orientacji (w KN); wzrost ten jest ograniczony przez odległości między dużymi wydzieleniami wzdłuż KN.

1. Introduction

Most alloys of commercial importance contain more than one phase. There is considerable interest in the use of second-phase particles to control both the grain size and the texture of alloys. The analyzed alloy contains both large ($> 1\mu m$) and small ($\ll 1\mu m$) particles. During deformation, zones of localized strain with characteristic local texture are formed in the neighborhood of large particles. The zones act as sites for PSN [e.g. 1, 2, 3]). Small particles pin the migrating boundaries, which highly reduces their mobility (*Zener pinning force*) and (probably) represses the differences in the migration rate between special and general boundaries. The recrystallization of such alloys with bimodal particle distribution has been analyzed extensively [e.g. 4]. There are no investigations, however, that would examine the recrystallization mechanisms on the basis of local crystallographic orientation measurements, especially in the zones of localized strain. This solution poses serious technical problems related to the measurement of orientations in highly deformed areas. The measurement of local orientation distributions in the TEM is the only method that allows such research to be realized. This paper focuses on the characterization of deformation microstructure — particularly of the zones of localized strain around large particles — and its behavior during annealing.

2. Experimental

The mechanisms of recrystallization structure and texture formation in alloys with the bimodal second phase particle distribution were investigated on the example of aluminum alloy 6013 (Table 1). The alloy was prepared by "Light Metals Division"

TABLE 1

Alloy 6013, chemical composition (% by weight)

Mg	Si	Cu	Mn	Fe	Others	Al
1.15	1.0	1.1	0.3	0.5	0.15	Remainder

in Skawina. The material, in the form of extruded flat bars, shows components typical for aluminum deformation texture, as Copper, S, Brass and Goss. Relatively uniform

dispersed particles were observed in the structure, both small ($\ll 1\mu$m) and large ($> 1\mu$m) ones. The crystallographic structures of some of the particles were described in [5, 6].

Samples for testing were supersaturated (kept for 1 hour at the temperature of 530°C), then aged at the temperature of 165°C for 5 days and reversible cold-rolled up to 75%.

Thin foils were prepared from sections perpendicular to the TD. Bright field images of the deformed state microstructure were obtained in the 200 KV TEM. The measurement technique described in [7, 8] was used to measure local crystallographic orientations of particular sites. In the next step, combined calorimetric–microscopic investigations were carried out. The release of stored energy was investigated by non-isothermal annealing [e.g. 9], with the help of the differential calorimeter. The spectrum of released stored energy consisted of several peaks. The samples were heated in the calorimeter to the defined temperatures of the peaks range and rapidly cooled down. The annealed samples were used to measure the topography of orientations of recrystallized grains by an EBSD technique in SEM/FEG. Sets of single orientations were used to calculate fractions of all sample symmetry related variants[1)] of particular components in the regions of the microstructure elements in question.

Global textures of the deformed and recrystallized stage were controlled through measurement with the X-Ray diffractometer of pole figures of {111}, {200}, {220} type, that were than used to calculate orientation distribution functions [10].

3. Deformed state

The cold-rolled texture showed features characteristic for deformation textures of materials with high stacking fault energies [e.g. 11]. The dominant orientations were scattered between the S and Copper components along the β-fibre. The Brass component was observed in the considerably weaker α-fibre, Fig. 1. The deformed structure was formed of wavy layers of microbands, lying roughly parallel to the rolling plane. In this lamellar structure there were dispersed small and large particles. The large particles break up the lamellar structure and create zones of localized strain around themselves, Fig. 2. In the deformation zones around large particles considerable scattering of orientations was observed; in an example in Fig 2 the eleven strong orientation changes on the distance of $\sim 4\mu$m are shown. A part of the orientations could be identified with the main deformation texture components rotated (by angles up to 40°) around the TD or/and ND. Moreover, a considerable fraction of the Cube component rotated around TD (TD_Cube) was also observed, Table 2.

[1)] In the case of a rolled polycrystalline sheet, the sample axes paralel to the normal (**ND**), transverse (**TD**) amd rolling directions (**RD**) can be interchanged according to the orthorhombic symmetry of rolling. Thus each compnent is represented by its Sample- Symmetry related Variants (**SSV**); the basic variant and three other generated by the two-fold axes $L^2_{ND}, L^2_{TD}, L^2_{RD}$, respectively.

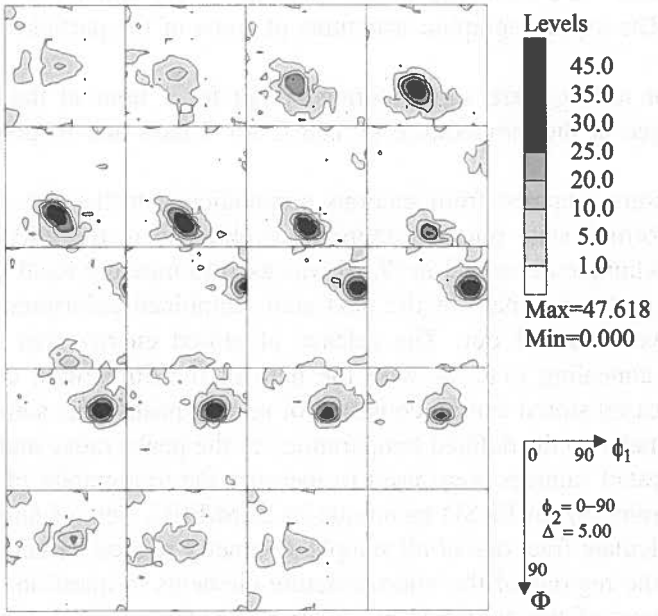

Fig. 1. Global texture of 6013 alloy after cold rolling to 75% reduction

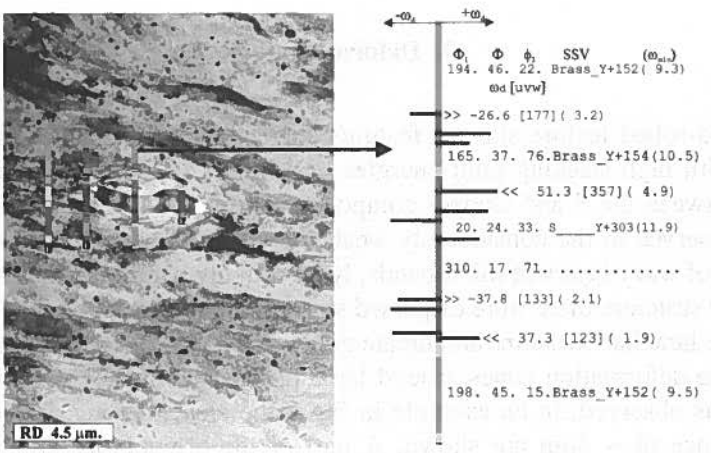

Fig. 2. Microstructure of 75% cold rolled 6013 alloy, longitudinal section, TEM. Changes of orientations in the zone of localized strain around large particle along 4 lines parallel to ND are shown. There are given some orientations (in Euler's angles ϕ_1, Φ, ϕ_2; letters with numbers indicate the SSV of particular components — as in the Table 2 — nearest to the measured orientations, the numbers in brackets give the disorientation angle ω_{min} from the particular component) as well as the orientation relationships (angle of disorientation ω_{min} and rotation [uvw]).

TABLE 2

The fractions of all SSVs of particular components in the set measured in the defined regions of microstructure of alloy 6013 after cold rolling up to 75%, a) The zones of localized strain around large particles, 970 orientations. New grains in deformed samples after heating in the calorimeter to: b) 330°C, d) 450°C. Orientations are given by symbols and in the Miller indices of the basic SSV (h k l)[u v w]. CopperY, S__Y, Brass__Y: +15, +30, −15, −30 indicate the particular orientation after rotation about the TD by +15°, +30, −15°, −30°, respectively; CopperZ, S__Z, Brass__Z indicate the particular orientation after rotation about the ND

Component		75% cold-rolled	heated to 330°C	heated to 350°C	heated to 450°C
Symbol	(h k l)[u v w]				
Goss	(0 1 1)[1 0 0]	0.5%	0.0%	0.1%	0.0%
ND-Goss	(0 1 1)[6 -1 1]	0.2%	0.0%	0.02%	2.6%
Brass	(0 1 1)[2 -1 1]	1.9%	0.2%	2.1%	0.9%
Copper	(1 1 2)[-1 -1 1]	2.6%	0.1%	0.1%	0.0%
S	(2 1 3)[-3 -6 4]	1.6%	1.7%	1.5%	6.7%
CopperY+15	~(1 1 4)[-2 -2 1]	0.4%	0.2%	3.0%	1.5%
CopperY−15	~(1 1 1)[-1 -1 2]	1.3%	0.8%	2.6%	1.3%
CopperY−30	(3 2 3)[-1 3 -1]	1.4%	0.2%	1.9%	2.0%
CopperY+30	(1 1 15)[-15 -15 2]	0.0%	0.3%	0.3%	3.6%
CopperZ−15	(1 1 2)[-2 -4 3]	0.7%	0.2%	3.2%	5.6%
CopperZ+15	(1 1 2)[-4 -2 3]	1.4%	0.1%	0.7%	1.7%
S__Y+30	(1 2 7)[15 -11 1]	4.7%	5.7%	9.0%	3.2%
S__Y+15	(7 1 15)[-7 -11 4]	7.0%	6.9%	4.5%	2.5%
S__Y−30	(10 7 10)[-6 10 -1]	2.5%	0.3%	6.1%	6.7%
S__Y−15	(10 7 10)[-3 10 10]	3.0%	16.6%	5.3%	4.9%
S__Z+15	(2 1 3)[-1 -1 1]	0.9%	5.7%	3.5%	3.0%
S__Z−15	(2 1 3)[-3 -15 7]	5.2%	0.4%	4.2%	5.8%
Braass__Y+30	(1 1 2)[1 -1 0]	4.3%	1.4%	4.5%	3.0%
Braass__Y+15	(1 3 4)[12 -8 3]	25.8%	42.9%	16.4%	3.9%
Braass__Z+15	(0 1 1)[7 -6 6]	2.1%	2.2%	1.5%	4.1%
Braass__Z−15	(0 1 1)[15 -4 4]	0.7%	0.0%	0.8%	0.7%
Cube	(0 0 1)[1 0 0]	0.3%	0.6%	1.0%	2.5%
RD__Cube__	(0 1 2)[1 0 0]	2.9%	1.5%	2.7%	3.6%
TD__Cube__	(0 2 3)[0 -3 2]	18.1%	3.6%	3.0%	5.6%
ND__Cube__	(0 0 1)[-3 1 0]	1.4%	0.3%	4.0%	4.9%
Total		91.1%	91.8%	82.4%	80.3%

4. Calorimetric examinations

The cold-rolled material was examined by non-isothermal annealing in the differential calorimeter. The spectrum of the released stored energy consisted of several

peaks. When the 75% cold rolled sample was heated at the rate of 10°C/min, one could observe three peaks in the following temperature ranges: ~326 – ~ 350°C, ~368 – ~ 486°C, ~ 492 – ~ 530°C, Fig. 3. In the next step, the samples were heated in the calorimeter to temperatures of the peaks ranges at the rates identical to those applied during non-isothermal examinations, and then cooled down immediately. In this paper the annealing behavior of samples annealed to the temperatures of the two first ranges were analyzed.

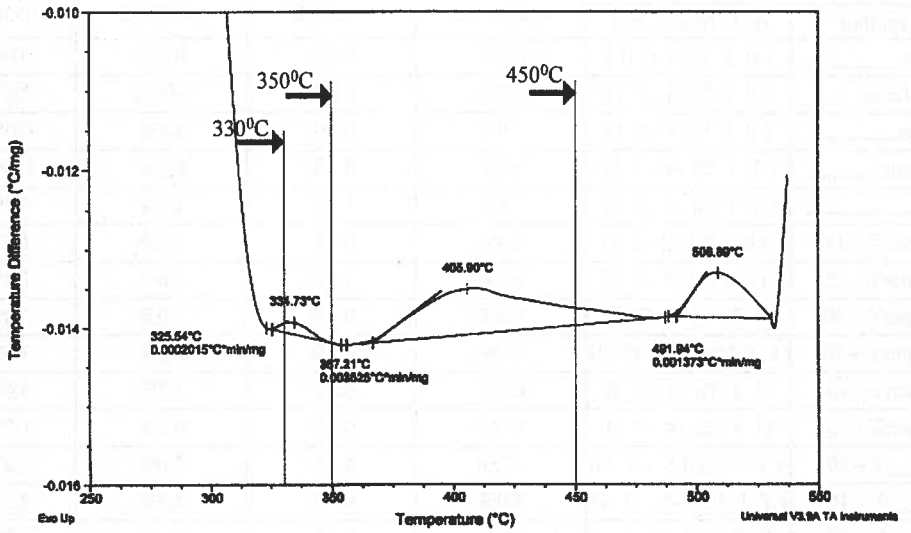

Fig. 3. Power difference, representing the release of stored energy from 75% cold-rolled 6013 alloy, as a function of annealing temperature

5. Microstructure and texture of partially and fully recrystallized samples

In samples heated to the temperature of 330°C (the range of the first peak) — one could observe nuclei / new grains that appeared mainly in the zones of localized strain around large particles by PSN, Fig. 4. Small and, initially, approximately equiaxial grains were distributed in bands parallel to the rolling plane, while the orientations of neighboring grains in a band were frequently close to each other. The distribution of orientations of new grains shows the same tendencies to group around rotated deformation components as in the case of the distribution measured in the zones of localized strain before heating (Table 2). In the sample heated to 350°C, the growth of new grains in the plane of the metal sheet can be observed. There appeared new grains, free from dislocations, whose lengths, along RD may exceed 50 , whilst their thickness did not exceed 4 (e.g. grain A in Fig. 5). In the temperature range of the first peak the growth in ND is absent or almost absent.

The fully recrystallized material can be obtained by heating a sample to the temperature of the end of the second peak, Fig. 6. Its structure contains both elongated grains and smaller ones, often almost equiaxial. The grains are now approximately 3 — 4 times thicker than those observed in the sample heated to 350°C. It can be infered that the temperature range of the second peak (Fig. 5) was dominated by the processes of migration of high angle grain boundaries (HAGB), formed within the temperature range of the first peak. As in the case of deformed material, the gradient of orientations in ND is considerably higher than in RD (Fig. 6 b, c). A very diffuse recrystalliza-

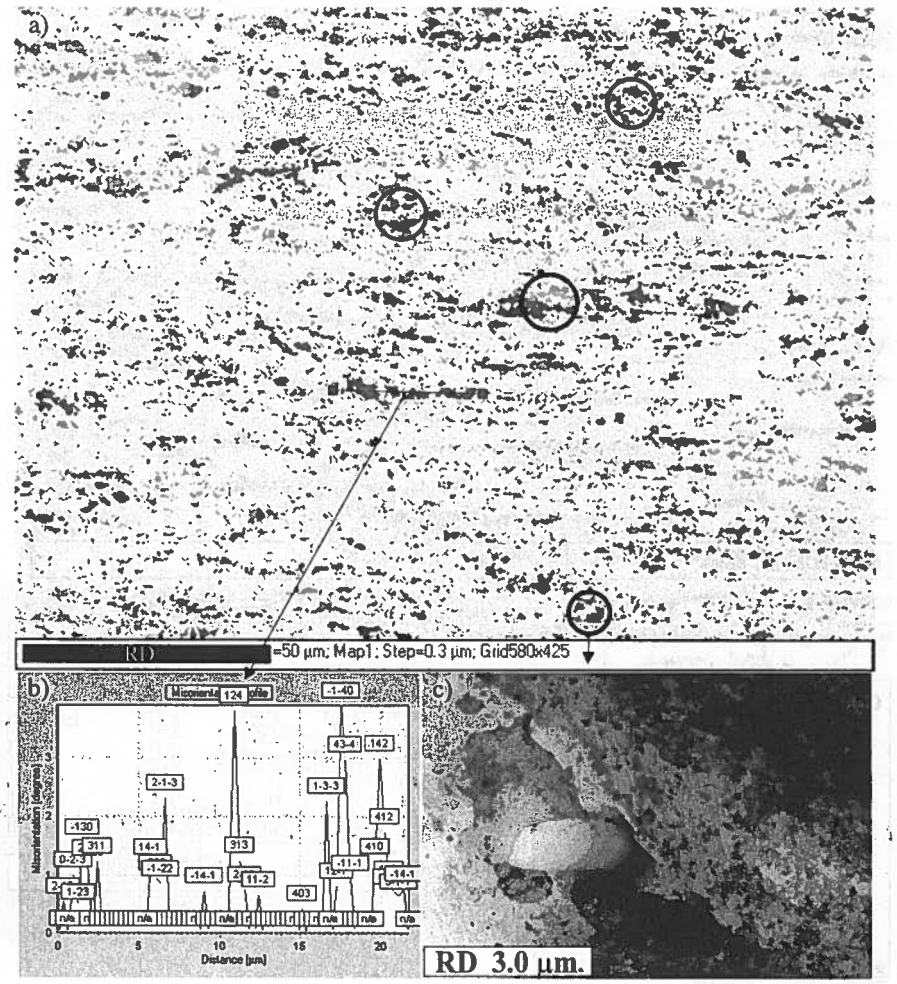

Fig. 4. Microstructure of 6013 alloy, 75% cold rolled and subsequently heated in the calorimeter to 330°C, longitudinal section, SEM/FEG. a) Orientation topography in areas of the new grains, deformed regions are bright gray. b) Example of disorientation profile along RD. c) Microstructure around a large particle of the second phase

tion texture reproduces roughly orientations of nuclei and new grains detected in the samples heated to the temperatures of the first peak range, Fig. 7 and Table 2.

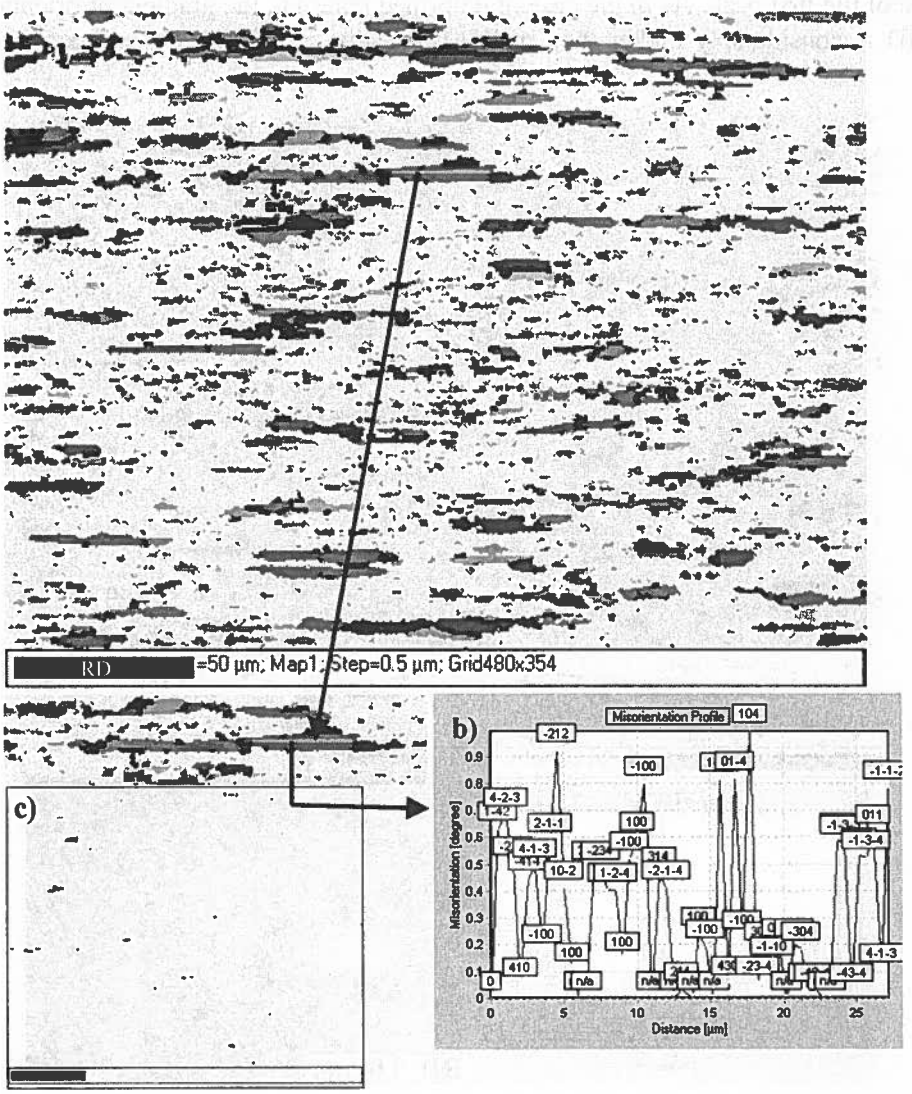

Fig. 5. Microstructure of 6013 alloy, 75% cold rolled and subsequently heated in the calorimeter to 350°C, longitudinal section, SEM/FEG. a) Orientation topography in areas of the new grains, deformed regions are bright gray. b) Example of disorientation profile along RD. c) Topography of new grains with orientations close to the Cube position

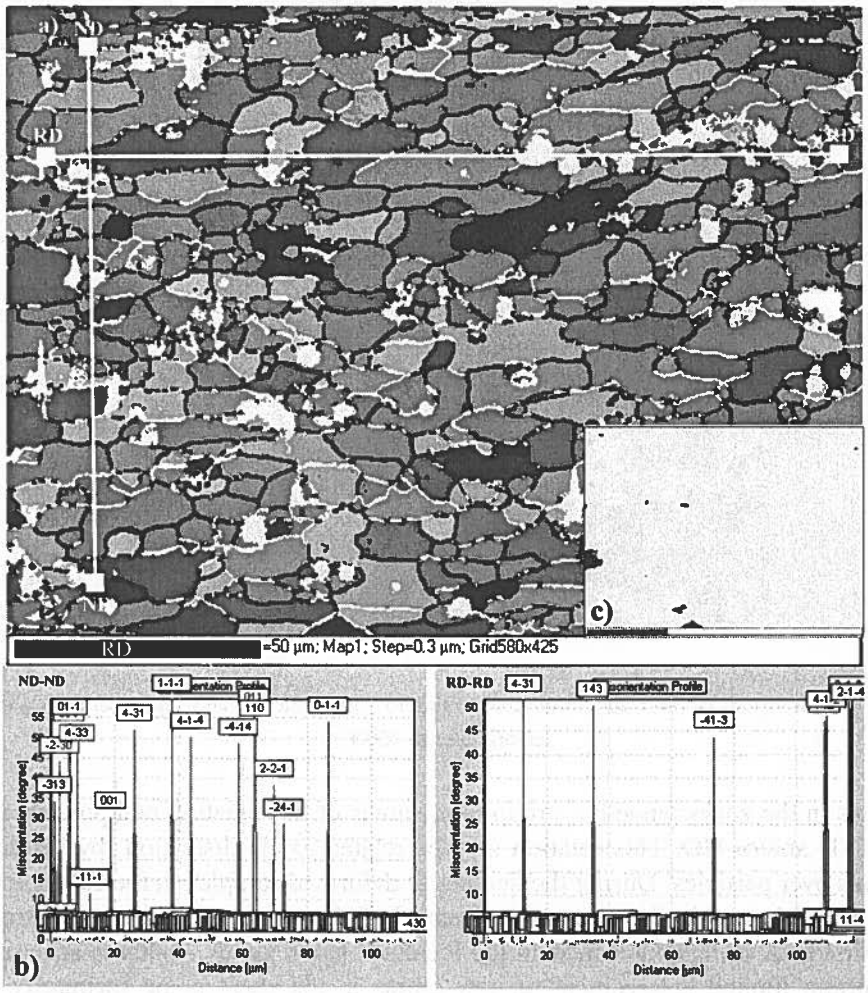

Fig. 6. Microstructure of 6013 alloy, 75% cold rolled and subsequently heated in the calorimeter to 450°C, longitudinal section, SEM/FEG. a) Orientation topography in areas of the new grains, b) Example of disorientation profile along the ND and the RD, respectively. c) Topography of grains with orientations close to the Cube position

6. Discussion

During deformation of aluminum alloy 6013 a typical ß-fiber rolling texture was developed, the main components being S and Copper, and a minor Brass (α-fiber) component, Fig. 1. The deformed matrix was structured as in a single-phase material (e.g. pure aluminum [12]) and consisted of subgrains and cells almost parallel to the rolling plane, highly elongated in RD. In the laminar structure, large (1 — 3μm) particles, surrounded by zones of localized strain, were dispersed. Strong diffused orientation dis-

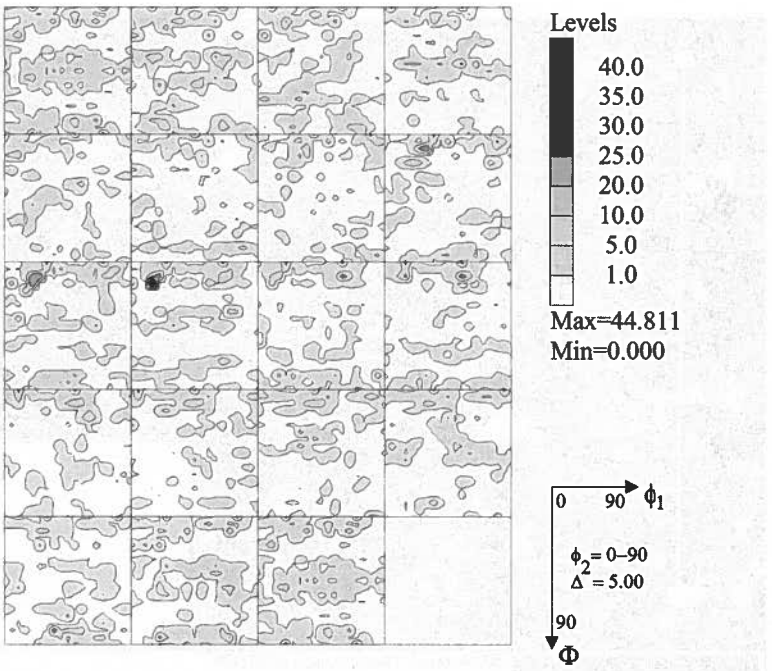

Fig. 7. Global texture of 6013 alloy after cold rolling to 75% reduction and subsequently heating the calorimeter to 450°C

tributions in the zones tended to group in the areas of deformation components rotated around TD and/or ND. This rotation may be related to the distortion (by bending) of subgrains over particles. During the heating of deformed samples in the calorimeter the energy was released in the spectrum consisted of three peaks. The temperature range of the first peak brings nucleation in the localized strain zones, which is accompanied by a certain limited enlargement of new grains in the sheet plane (primarily in the direction parallel to RD). The formation of grains highly elongated in RD may be correlated to the processes of local recovery [13], triggered in the zones of distorted subgrains in proximity of large particles, that continued to develop along the bands of the deformed matrix in the directions of low orientation gradients. Elongated grains appear due to the annihilation of low angle grain boundaries (LAGB) between chains of subgrains / nuclei. No growth in ND (subgrain thickening) — characteristic for the recrystallization of pure aluminum — was observed in the temperature range of the first peak. The orientations of new grains were located in the area of scattering around orientations measured before annealing in the zones of localized strain. Infrequent new grains with orientations approaching Cube component were also observed. The nuclei of these grains appeared most probably in the deformed matrix (as in the case of pure aluminum), and not in the zones around particles. The material recrystallized fully after heating the sample to the temperature of the end of the second peak. The structure was still dominated by grains elongated in the RD. However, equiaxial grains

were also identified. In a very diffuse texture, one can find orientations from the area of deformation texture rotated around the TD and ND by angles from 0 to ~ 40° and a small amount of orientations scattered around Cube component, Fig. 7. The distances between HAGBs in ND (grain thicknesses) corresponded approximately to the distances between the bands of elongated new grains in the sample heated to the temperature of the end of the first peak, and they were determined by the distances along ND between large particles. Therefore, one can assume that HAGBs migration, formed in the temperature range of the first peak, was the main process in the temperature range of the second peak. This migration, mostly in the ND, was limited to "free areas" of the deformed matrix between bands of new grains formed in the zones of localized strain in the initial stage of recrystallization (in the temperature range of the first peak). It is here important to note that the size of the infrequent grains with orientations close to the Cube component does not differ from the size of grains with other orientations. The growth of Cube oriented grains in pure aluminum is related to the mechanisms of selected growth [14, 15]. **The factor preventing selective growth in alloy 6013 is found in the combined effects of small and large particles;** the first highly reduce HAGB mobility due to particle pinning and (probably) repress the differentiation of migration rates between the general and special HAGBs (those that can be described by the relation $35 \div 50°$ $\sim<111>$ [12, 16], and that are responsible for intense growth of Cube-oriented grains). In general slowed-down movement of HAGBs makes it possible for new generations of nuclei with orientations that are not privileged by mechanisms of oriented growth to enter into "play" and to grow. On the other hand the migration of HAGB, mostly in the ND, is limited to "free areas" of the deformed matrix between bands of new grains formed in the zones of localized strain in the initial stage of recrystallization. The combined effect of both mechanisms leads to the structure refinement and randomization of texture, Figs 6 and 7.

7. Conclusions

1. The deformed structure of aluminum alloy 6013 is formed of wavy layers of microbands consisting of elongated subgrains and cells that are almost parallel to the rolling plane. The texture of the laminar matrix is dominated by deformation components S, Copper and Brass. In the matrix, large, second-phase particles ($1 \div 3\mu$m) are dispersed, surrounded by zones of localized strain. The strong scattered orientations of the zones tend to group around deformation components rotated around TD and/or ND.

2. Recrystallization of the material develops in two stages.

a. In the first stage, recrystallization process proceeds in highly deformed zones in the vicinity of large particles. Observations identified a certain limited enlargement of new grains, but only in the directions parallel to the metal sheet plane. The orientation distribution of new grains contained orientations measured before annealing in the zones.

b. Observation of the second stage of recrystallization identified grain thickening, while the final grain thickness is limited by the distances between large particles along ND, dependent on a degree of cold rolling.

Acknowledgements

Financial support from the State Committee for Scientific Research (KBN — 7T08A 054 21) is gratefully acknowledged.

REFERENCES

[1] F.J. Humphreys, M. Hatherly, Recrystallization and Related Annealing Phenomena, Pergamon Press, Oxford, 235 (1996).
[2] F.J. Humphreys, Metal Sci., **13**, 136-145 (1979).
[3] M.G. Ardakani, F.J. Humphreys, Acta metall. mater. **42**, 763-780 (1994).
[4] E. Nes, Acta Metall. **24**, 391-398 (1976).
[5] L. Lityńska, R. Sholtz, J. Dutkiewicz, Proc. XVIII Conf. Applied Crystalography, ed. H.Morawiec & D.Stróż, World Scientific, 346-349 (2001).
[6] C. Barbosa, J.M.A. Rebello, O. Acselrad, J. Dille, J.-L. Delplanke, Z. Metallkd. **93**, 208-211 (2002).
[7] A. Morawiec, J.J. Fundenberger, E. Bouzy & J.S. Lecomte, J. Appl. Cryst. **35**, 287 (2002).
[8] J.J. Fundenberger, A. Morawiec, E. Bouzy & J.S. Lecomte, Ultramicroscopy **96**, 127-137 (2003).
[9] W.F. Hemminger, Cammenga, Methoden der Thermischen Analyse, Springer-Verlag 1989.
[10] LabSoft 2003, LaboTex v. 2.1.016 the texture analysis software package LabSoft s.c.
[11] O. Engler, J. Hirsch, K. Lücke, Acta Metall. **37**, 2743- 2753 (1989).
[12] K. Sztwiertnia, Mater. Sci. Forum, **426 – 432**, 3721-3726 (2003).
[13] R.D. Doherty, J. Szpunar, Acta Metall. **32**, 1789-1798 (1984).
[14] K. Sztwiertnia, F. Haessner, Proc. of 16th RisØ International Symposium on Materials Science: **Microstructural and Crystallographic Aspects of Recrystallization**, ed. by N. Hansen, D. Juul Jensen, Y. L. Liu, B. Ralph, RisØ National Laboratory, Denmark, 565-571 (1995).
[15] K. Sztwiertnia, Archives of Metall. **41**, 101-116 (1996).
[16] B. Liebmann, K. Lücke, G. Masing, Z. Metallkde **47**, 57 (1956).
[17] O. Engler, J. Hirsch, Mater. Sci. Forum 217-222, 479-486 (1996).
[18] R.K. Singh, A.K. Singh, Scripta Mater. 38, 1299-1306 (1998).

Received: 27 January 2005.